Sensors and Materials, Vol. 13, No. 6 (2001) 343–350
MYU Tokyo

S & M 0454

Monte Carlo Simulation of Wet Chemical Etching of Silicon

Erik van Veenendaal[1], Jaap van Suchtelen[1,2], Paul van Beurden[1], Herma M. Cuppen[1], Willem J. P. van Enckevort[1], A. Jasper Nijdam[2], Miko Elwenspoek[2] and Elias Vlieg[1]

[1]RIM Dept. of Solid State Chemistry, University of Nijmegen,
Toernooiveld 1, 6525 ED Nijmegen, The Netherlands
[2]MESA+ Research Institute, University of Twente, P.O. Box 217,
7500 AE Enschede, The Netherlands

(Received September 1, 2000; accepted December 1, 2000)

Key words: Monte Carlo simulation, surface micromorphology, orientation-dependent etch rate

The aim of this paper is to demonstrate that Monte Carlo simulation can be a powerful tool to understand wet chemical etching of silicon. We have performed Monte Carlo simulations of etching of three important silicon surfaces: Si(111), Si(100) and Si(110). Interpretation of these simulations yields an understanding of the micromorphology of etched silicon surfaces and the orientation dependence of the etch rate.

1. Introduction

All microscopic features on etched silicon surfaces are the result of etching mechanisms working on an even smaller length scale, the atomic length scale. Using Monte Carlo methods, it is possible to simulate etching of silicon on this length scale. That is why, in spite of all imperfections and necessary assumptions, Monte Carlo simulations are worthwhile: they facilitate and inspire discussions on the atomic scale etching mechanisms.

We have used Monte Carlo simulation to study wet chemical etching of silicon in potassium hydroxide (KOH). First, we studied the etch rate anisotropy for vicinal Si(111) surfaces.(1) The $Si(\bar{1}\bar{1}1)$ surface is dominated by etchpits, induced by stacking faults,(2,3) whose shape reflects the anisotropy. Second, we investigated the effect of a mask junction, which is encountered in underetching experiments.(4) Finally, we studied the formation and

stabilisation of pyramidal protrusions on the Si(100) surface, which occur at low KOH concentrations,[5] and the staircase or zigzag pattern on the Si(110) surface, which is the dominant feature except at very high KOH concentrations.[6]

2. Monte Carlo Method

The silicon crystal is reduced to a diamond cubic lattice of silicon atoms connected by nearest-neighbor bonds. For Si(111), Si(100) and Si(110), it is possible to divide a crystal interface into an array of columns of atoms perpendicular to the surface. On these columns the solid-on-solid (SOS) condition, which excludes overhangs, is imposed. This allows a representation of the surface by an array of integers denoting the heights of the topmost atoms in each column. As etching of silicon is an irreversible process, the only elementary process we need to consider is the removal of the top layer of atoms. The annihilation probability to remove an atom is determined by the surface configuration directly around the atom, i.e., the number and direction of nearest-neighbor bonds with the bulk of the crystal. The annihilation probability changes if the atom is adjacent to a mask junction or if the atom is shielded by a microscopic particle on the surface that acts as a semipermeable mask. A Monte Carlo program for etching is no more than an iteration of a procedure that chooses the removal of an atom out of all possible annihilations with a probability proportional to its annihilation probability.

3. The Si(111) Surface

3.1 *Etch rate anisotropy*

We distinguish between annihilations of adatoms (1 bond), kink atoms (2 bonds), step atoms (3 bonds, 1 vertical) and terrace atoms (3 bonds, all in plane). Monte Carlo simulations result in smooth surfaces and anisotropic etching, if the differences between the annihilation probabilities for removal of atoms from kink, step, and terrace sites are sufficiently large. Then, etching on the exact Si(111) surface proceeds through birth and spread of monolayer etchpits. We have derived a simple model that accounts for this birth-and-spread mechanism. Etching of vicinal Si(111) surfaces proceeds through birth-and-spread and misorientation step flow. We have developed a model for the interaction of these processes to obtain the etch rate as a function of the misorientation.[7,8] Combination with the birth-and-spread model yields an expression for the etch rate with the annihilation probabilities as only variables. For a number of different choices for the annihilation probabilities, Monte Carlo simulations confirm this analytical etch rate function. The analytical expression for the etch rate as a function of misorientation can also be used to fit experimental etch rates for etching of vicinal Si(111) in KOH. In Fig. 1 we have fitted the experimental etch rate for 26 wt% KOH at 70°C obtained in a hemisphere etch experiment by Sato *et al.*[9]

In the derivation of the analytical etch rate function, we also automatically obtain an analytical expression for the velocity of steps on the Si(111) surface as a function of the orientation of these steps. This step velocity function can be used to calculate the

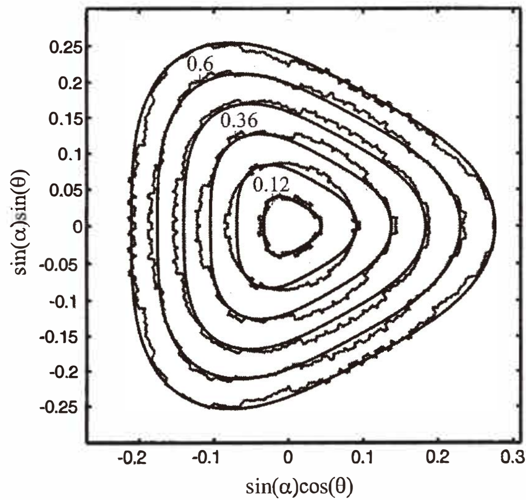

Fig. 1. Contour plot of the etch rate for vicinal Si(111) etched in 26 wt% KOH at 70°C in μm/min [courtesy of K. Sato]. Angle α is the misorientation of the surface and angle θ is the step orientation. The smooth lines correspond to the analytical etch rate function.

microscopic shape of stacking-faults-induced etch pits, using the Gibbs-Wulff construction.[10] We substituted the fitted values for the annihilation probabilities of Fig. 1 in the expression for the step velocity. In Fig. 2(a), the orientation dependence of the step velocity is given. The corresponding Gibbs-Wulff shape is also drawn. In Fig. 2(b), we compared this calculated shape with the shape of an etch pit observed on a {111} surface on the exact same hemisphere used to obtain the orientation dependence of the etch rate. It is apparent that both shapes agree quite well.

3.2 *Influence of a mask junction*

We have studied etching of the (100) surface of a simple cubic crystal that is bounded by a mask. It is assumed that the annihilation probability of an atom solely depends on the energy required to break all nearest-neighbor bonds with the crystal (bond strength ϕ/kT) and, if the atom is adjacent to the mask, the one bond with the mask (bond strength ϕ_{mask}/kT).

Monte Carlo simulations show that, if ϕ_{mask}/kT is smaller than ϕ/kT, the mask junction acts as a velocity source;[11] a small facet is nucleated at the mask junction (see Fig. 3). In underetching experiments it is indeed found that etching of Si(111) can be accelerated by preferred nucleation of steps at the mask junction.[4]

We have modeled the nucleation behavior at the mask junction and have found that the misorientation of the nucleated facet only depends on the interaction of the crystal with the mask, ϕ_{mask}/kT, and not on the interaction between atoms in the bulk of the crystal, ϕ/kT.

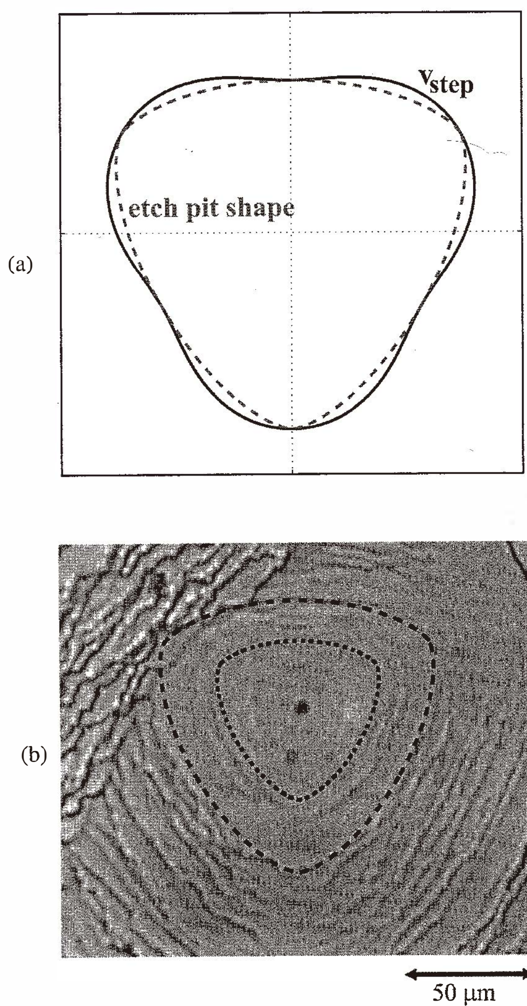

Fig. 2. (a) The step velocity on Si(111) corresponding to the etch rate of Fig. 1 and the expected shape of etch pits on Si(111). (b) Etch pit on Si(111) etched in 26 wt% KOH at 70°C. The dashed lines correspond to the expected shape of etch pits.

4. Micromorphology of Si(100) and Si(110) Surfaces

The most striking feature in the micromorphology of silicon surfaces with an orientation in the range between Si(100) and Si(110) is the occurrence of protrusions, ranging from pyramidal etching hillocks on Si(100) to staircase or zigzag structures on Si(110).

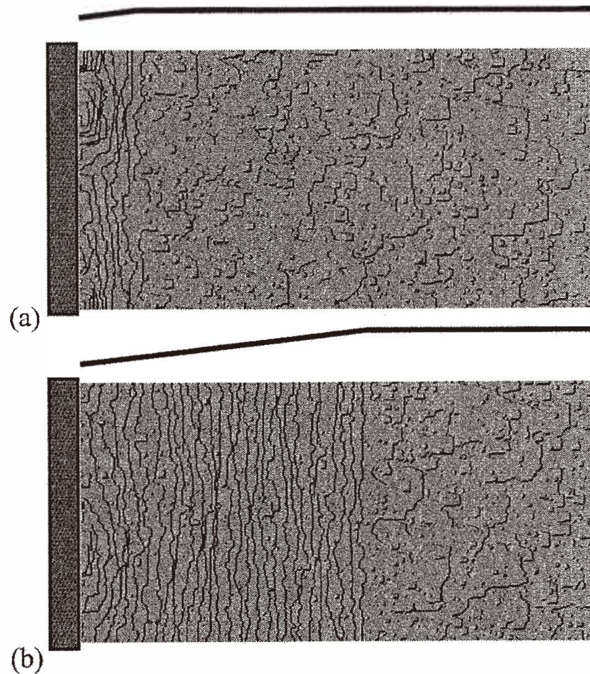

Fig. 3. Side and top view of a simple cubic (100) surface simulated with ϕ/kT=2 and ϕ_{mask}/kT=1 after etching of (a) 100 and (b) 600 atomic layers.

Our hypothesis is that all these structures are a result of the same mechanism, namely the presence of a particle on the top of each protrusion. This particle acts as a semipermeable mask, locally decreasing the etch rate. The nature of this semipermeable masking particle is unknown but it may very well be a silicate particle that is produced during etching. This has actually been suggested in the literature for the case of the pyramids on Si(100).[12,13]

We have performed Monte Carlo simulations of etching of Si(100) and Si(110) surfaces with a semimask placed on the surface that covers four columns of atoms. Again, we assume that the annihilation probability of an atom only depends on the number of nearest-neighbors (1, 2 or 3) and further, we assume that for the top atoms of the columns underneath the semimask, the probability is reduced by an efficiency factor e.

These simulations indeed yield pyramidal hillocks on Si(100) that resemble experimentally found etching hillocks (see Fig. 4). Simulations of etching of Si(110) in the presence of a semimask yield a zigzag structure (see Fig. 5). This structure only superficially resembles an experimental zigzag structure, for which the protruding edge is parallel to <110>.

There is an important difference between the orientation dependence of the etch rate of the Monte Carlo simulations resulting from our choice of the annihilation probabilities and

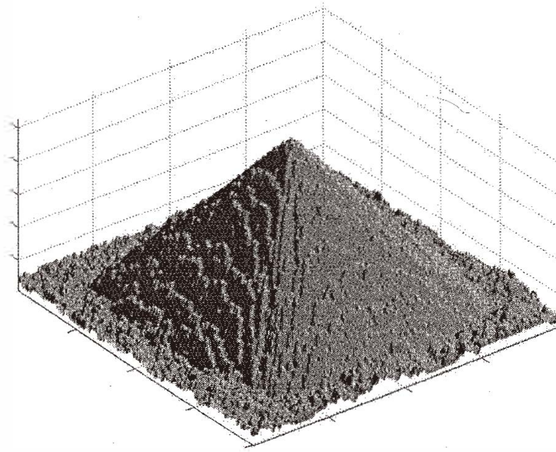

Fig. 4. Pyramidal etching hillock on Si(100) formed underneath a semimask simulated with e = 0.01.

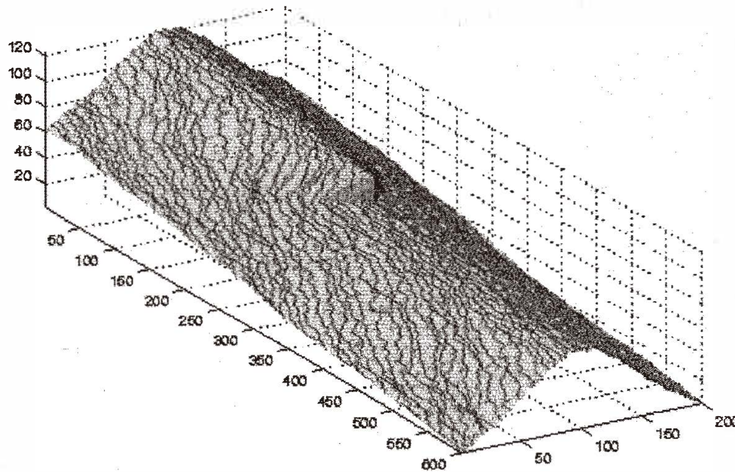

Fig. 5. Zigzag structure on vicinal Si(110), 6° misorientation towards (100), formed underneath a semimask simulated with e = 0.01.

the orientation dependence of the etch rate in KOH etching experiments. For the simulations, the etch rate of Si(100) is a maximum, while experimentally the etch rate of Si(100) is a local minimum and, just as important, the etch rate for Si(110) is larger or not much smaller than the etch rate for Si(100). This implies that a particle on the top alone is not

sufficient to stabilise a pyramidal etching hillock. Our conclusion is that the edges of the pyramids and the protruding edges of the zigzag structures must also be stabilised by some mechanism. We hypothesise that this stabilisation of the edges is the direct consequence of the presence of the particles on the tops of the protrusions. Apart from the large particles on the top there are numerous smaller particles present on the surface that do not affect the etch rate significantly and tend to move perpendicular to the local surface. This indicates that protruding edges act as sinks of these small particles. Larger particles are assembled on these edges, which decreases the etch rate of the edges.

5. Conclusions

Using Monte Carlo simulations we have studied different aspects of etching of the important silicon surfaces in KOH. These Monte Carlo simulations provide valuable insight into the atomic-scale origins of the "mesoscopic" corrugations found on etched silicon surfaces: triangular etch pits on Si(111), pyramids on Si(100) and zigzag patterns on Si(110).

Acknowledgements

We gratefully acknowledge Professor K. Sato of Nagoya University for providing the experimental silicon etch rate data. This work is supported by the Dutch Technology Foundation (STW).

References

1 E. van Veenendaal, P. van Beurden, W. J. P. van Enckevort, E. Vlieg, J. van Suchtelen and M. Elwenspoek: J. Appl. Phys. **88** (2000) 4595.
2 T. Muller, T. Feichtinger, B. Funkhauser, A. C. Benkitsch, O. Brand and H. Baltes: Proc. MME'98 (1998) p. 59.
3 A. J. Nijdam, J. G. E. Gardeniers, C. Gui and M. Elwenspoek: Sensors & Actuators A **86** (2000) 238.
4 A. J. Nijdam, J. W. Berenschot, J. van Suchtelen, J. G. E. Gardeniers and M. Elwenspoek: J. Micromech. Microeng. **9** (1999) 135.
5 S.-S. Tan, M. L. Reed, H. Han and R. Boudreau: J. Micromech. Microeng. **4** (1994) 147.
6 K. Sato, M. Shikida, T. Yamashiro, M. Tsunekawa and S. Ito: Sensors & Actuators A **73** (1999) 122.
7 J. van Suchtelen and E. van Veenendaal: J. Appl. Phys. **87** (2000) 8721.
8 E. van Veenendaal, J. van Suchtelen, W. J. P. van Enckevort, K. Sato, A. J. Nijdam, J. G. E. Gardeniers and M. Elwenspoek: J. Appl. Phys. **87** (2000) 8732.
9 K. Sato, M. Shikida, Y. Matsushima, T. Yamashiro, K. Asaumi, Y. Iriye and M. Yamamoto: Sensors & Actuators A **64** (1998) 87.
10 P. Bennema and J. P. van der Eerden: Morphology of Crystals, part A, ed. I. Sunangawa, (Terrapub, Tokyo, 1987) p. 385.
11 J. van Suchtelen, A. J. Nijdam and E. van Veenendaal: J. Crystal Growth **198–199** (1999) 17.

12 L. M. Landsberger, S. Naseh, M. Kahrizi and M. Paranjape: J. Microelectromech. Syst. **5** (1996) 106.
13 U. Schnakenberg, W. Benecke and P. Lange: Tech. Dig. Transducers '91, (San Francisco, 1991) p. 815.